

Up and down wave separation of multicomponent data at the ocean bottom

Chanpen Silawongsawat and Gary F. Margrave

ABSTRACT

An elastic modelling program (Elmo) has been modified to generate multicomponent synthetic seismic data at the ocean bottom. The program is also able to fully separate P and S into their up or down subset. A proposed scalar-combination method to separate up and down coming waves at the ocean bottom is then tested with this synthetic data. The scalar relationship between the vector wavefield of particle velocity and the scalar wavefield of pressure based on Hooke's law is reviewed. With total measurement of downcoming wave accounted for, the expressions to combine the ocean bottom multicomponent data for the upcoming waves in each component are restated. Some synthetic results for different definitions of up and down wave separation are produced. The results of the scalar combination method for each component are shown to have successfully separated up and downcoming waves.

INTRODUCTION

An up-down wave separation method, called *scalar combination*, for ocean bottom seismic (OBS) data was proposed previously (Silawongsawat and Margrave, 1999). It was developed as a preparatory step prior to a P-S mode separation method at the ocean bottom presented by Donati (1996). General up-down wave separation also causes suppression in water column of receiver-side multiples.

In conventional surface seismic there are only arrivals from below which we call upcoming waves, possibly both P and S, Figure 1(a). The OBS system also takes downcoming P wave into account, Figure 1(b). Let subscripts *u* and *d* indicate up and down incident waves. α , β and ρ are P- and S-velocity and density of a notified medium, respectively. Let z_0 and z_1 be the depth of the land or ocean surface and seafloor.

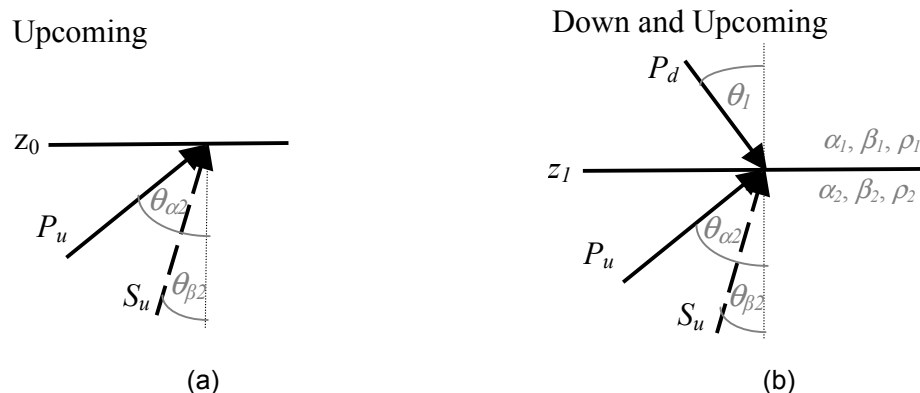
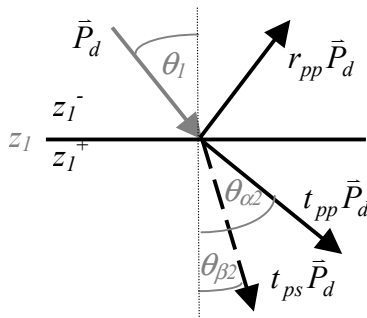


Figure 1. (a) Possible incident waves in surface seismic: upcoming waves. (b) Possible incident waves in OBS: down and upcoming. All waves have the same ray parameter.

The receivers in both systems are usually situated at the top of the earth layer where is either a gas-solid or liquid-solid interface. Seismic measurement there always includes scattered waves for each arrival. Figure 2 shows scattered waves of a downcoming P and Figure 3 scattered waves of the upcoming P and S. These resultant waves, up- and downgoing, can be calculated from their incident waves, up- and downcoming, as also shown. Thus the OBS data, as shown in Figure 1(b), is a combination of all possible waves: upcoming, downcoming, upgoing and downgoing from both diagrams in Figure 2 and 3,

$$OBS\ data = \bar{P}_U + \bar{S}_U + \bar{P}_D = \bar{U} + \bar{D} \quad (1)$$

where U and D indicate total measurement of both incident and scattered waves. The 4-component OBS system complicates the matter furthermore because the total measurement can be taken either above (by hydrophone) or below (by 3C geophone) the interface. Let r_{pp} , t_{pp} and t_{ps} be P-P reflection, P-P and P-S transmission coefficients of the ocean bottom for displacement. Then:



The total measurement of downcoming P, \bar{P}_D , is

Above the seabed:

$$\bar{P}_D(z_1^-) = (1 + r_{pp})\bar{P}_d \quad (2)$$

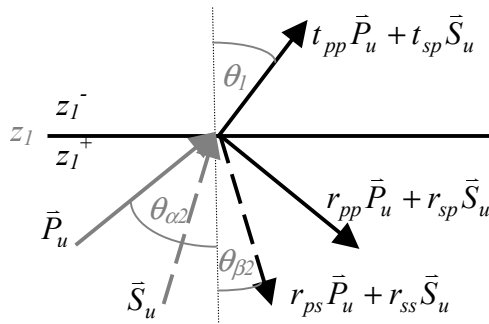
Below the seabed:

$$\bar{P}_D(z_1^+) = (t_{pp} + t_{ps})\bar{P}_d \quad (3)$$

Note that $\bar{P}_D(z_1^-) \neq \bar{P}_D(z_1^+)$ in general.

Figure 2. Scattering waves of the downcoming P.

The superscripts $-$ and $+$ of z_l indicate levels just above and just below the seafloor, respectively.



The total measurement of upcoming P and S

Above the seabed:

$$\bar{P}_U(z_1^-) + \bar{S}_U(z_1^-) = t_{pp}\bar{P}_u + t_{sp}\bar{S}_u \quad (4)$$

Below the seabed:

$$\begin{aligned} \bar{P}_U(z_1^+) + \bar{S}_U(z_1^+) = & (1 + r_{pp} + r_{ps})\bar{P}_u \\ & + (1 + r_{sp} + r_{ss})\bar{S}_u. \end{aligned} \quad (5)$$

Figure 3. Scattering waves of the upcoming P and S.

Considering the reaction just above the ocean bottom in Figure 2, only P-waves exist in the water. Thus above the seafloor, there is only a reflected P as a scattered wave from a downcoming incident P wave. The scattered waves are written in terms of their appropriate incident waves. Therefore the measurement can then be written in terms of the incident wave as in Equation (2), and equation (3)-(5) are the total downcoming waves below the seafloor, the total upcoming above and below the seafloor, respectively. They decompose each element of OBS data from Equation (1) into incident and scattered waves for receivers above or below the seafloor. The subscripts D and U denote total measurement of a wave which includes scattered waves at an interface, or so called interface effects. This is contrasted with u and d which denote a pure up or down incident wave. For example, the total measurement of a downcoming wave above the seafloor, equation (2), has therefore contained also up and down propagating waves. The term up and down wave separation can then be confusing.

REVIEW OF SCALAR COMBINATION METHOD

Particle velocity and pressure relationship

A relationship between the scalar wavefield pressure, w , and the vector wavefield particle velocity, \bar{v} , through the equation of motion is

$$\bar{\nabla} w = \rho \frac{\partial \bar{v}}{\partial t} \quad (6)$$

where ρ is density. Noticeably, this is a dynamic vector equation. Its vertical component gives the expression for the vertical velocity as a function of the pressure (Amundsen, 1993). Barr and Sanders (1989) used this result in their method for the elimination of water column reverberations. However, in a general case, according to Sheriff and Geldart (1995, p.38), pressure is proportional to the fractional volume change, or dilatation, through

$$w = -\kappa \bar{\nabla} \cdot \bar{u} \quad (7)$$

where κ is the bulk modulus given for 2D by

$$\kappa = \rho(\alpha^2 - \beta^2) \quad (8)$$

or for 3D

$$\kappa = \rho(\alpha^2 - \frac{4}{3}\beta^2) \quad (9)$$

Thus taking a time derivative of equation (7) to get particle velocity, this equation becomes

$$\frac{\partial w}{\partial t} = -\kappa \bar{\nabla} \cdot \bar{v} \quad (10)$$

This is a scalar equation, which shows how a combination of all velocity components relates to the pressure. Consider the relationships between P and \bar{v} expressed in equations (6) and (10). They are derived from two independent physical laws (Newton's and Hooke's laws) which, taken together, lead to the elastic wave equation. So if they are combined, the wave equation (or the dispersion relation) will result. They describe the relationships between the scalar wavefield pressure and the vector wavefield particle velocity in two different ways. Equation (6) states how the pressure individually relates to each velocity component. Alternatively, equation (10) is obtained from Hooke's law and relates pressure with a combination of all velocity components. In brief, the equation of motion connects the pressure and particle velocity as vectors whereas Hooke's law leads to a scalar relationship.

We can expand (10), for 2D, into horizontal and vertical (x and z) components as

$$\frac{\partial w}{\partial t} = -\kappa \left(\frac{\partial v_x}{\partial x} + \frac{\partial v_z}{\partial z} \right) \quad (11)$$

Taking a double-spatial Fourier transform over x and z on equation (11) and separating upward and downward travelling waves, we have

$$i\omega W = -\kappa (ik_x X + ik_z Z^+ - ik_z Z^-) \quad (12)$$

where $W = F(w)$, $X = F(v_x)$ and $Z = F(v_z)$. Also the superscript $+$ denotes a wavefield that propagates in the increasing z direction, downward travelling in depth, and $-$ denotes an upward traveling wavefield. Equation (12) can be rewritten as

$$W = -\kappa (pX + qZ^+ - qZ^-) \quad (13)$$

where p and q are horizontal and vertical slowness given by

$$p = \frac{k_x}{\omega} = \frac{\sin \theta}{\alpha} \quad \text{and} \quad q = \frac{k_z}{\omega} = \frac{\cos \theta}{\alpha} \quad (14)$$

ω is the temporal frequency and θ is the wave propagation angle. The spatial derivative depends on the direction of wave propagation in relation to the direction of the derivative. Accordingly, the vertical component, $\frac{\partial v_z}{\partial z}$, is split into two separate terms for upward and downward travelling waves as shown. For simplification, we consider only the positive offset of a record.

Equation (13) is the starting point for a method that includes the horizontal and vertical components for separation of upcoming and downcoming wavefields.

Interface effects for downcoming waves

Referring to Figure 2 and equation (2), the hydrophones would detect $(1+r_{pp})W_d$ as the sum of incident and reflected waves above the ocean bottom,

$$W_D(z_1^-) = (1+r_{pp})W_d, \quad (15)$$

where the d subscripts an incident downcoming wave.

The particle velocity field is measured, by the geophones that couple with the earth layer, below the seafloor. The geophone would record a sum of transmitted P and transmitted S, $(t_{pp}+t_{ps})P_d$, as in equation (3) which can be decomposed into the horizontal component as

$$X_D(z_1^+) = (\sin\theta_{\alpha 2}t_{pp} + \cos\theta_{\beta 2}t_{ps}) \frac{X_d}{\sin\theta_{\alpha 1}}, \quad (16)$$

or
$$X_D(z_1^+) = \varepsilon X_d, \quad (17)$$

where
$$\varepsilon = \frac{\alpha_2}{\alpha_1}t_{pp} + \frac{\cos\theta_{\beta 2}}{\sin\theta_{\alpha 1}}t_{ps} = \frac{\alpha_2}{\alpha_1}t_{pp} + \frac{\beta_2 q_{\beta 2}}{\alpha_1 p}t_{ps}. \quad (18)$$

The vertical component of the particle velocity is continuous across the liquid-solid interface. Therefore it can be expressed as a vertical decomposition of equation (2),

$$Z_D(z_1^+) = Z_D(z_1^-) = (1-r_{pp})Z_d, \quad (19)$$

Equation (13) is valid for the total pressure and velocity wavefields at some position and time. However, it is simpler to work with the incident wavefields individually. This gives

$$W_d = -\kappa_1(pX_d + qZ_d) = -\rho_1\alpha_1(\sin\theta_{\alpha 1}X_d + \cos\theta_{\alpha 1}Z_d) \quad (20)$$

Then, substitute into equation (20) the expressions for the incident wave as a function of the total measurement of each component from (15), (17) and (19). This becomes

$$\frac{1}{1+r_{pp}}W_D = -\rho_1\alpha_1\left[\frac{\sin\theta_{\alpha 1}}{\varepsilon}X_D + \frac{\cos\theta_{\alpha 1}}{1-r_{pp}}Z_D\right]. \quad (21)$$

This expression relates the total downcoming of pressure field to the velocity components.

Elimination of downcoming wave

At the liquid-solid interface, all receiver responses can be described in terms of their up and down arrivals including their scatterings from equation (1), Figure 2 and 3 as

$$W(z_1) = W_U(z_1^-) + W_D(z_1^-) \quad (22)$$

$$X(z_1) = X_U(z_1^+) + X_D(z_1^+) \quad (23)$$

$$Z(z_1) = -Z_U(z_1^+) + Z_D(z_1^+) \quad (24)$$

The up and down terms in (22)-(24) are independent of each other. However, only the vertical component is sensitive to the up-down direction of propagation. Due to this difference in sign conventions for up and down travelling waves in vertical component, the downcoming arrivals for pressure, vertical and horizontal components can be eliminated. Thus, substituting downcoming waves in terms of the total and upcoming waves from (22)-(24), into (21) yields

$$\frac{1}{1+r_{pp}}(W - W_U) = -\rho_1\alpha_1\left[\frac{\sin\theta_{\alpha 1}}{\varepsilon}(X - X_U) + \frac{\cos\theta_{\alpha 1}}{(1-r_{pp})}(Z - Z_U)\right] \quad (25)$$

Multiply by (1+r_{pp}) to solve for pressure

$$W_U = W - \alpha_1\rho_1\left[\frac{1+r_{pp}}{\varepsilon}\sin\theta_{\alpha 1}(X - X_U) + \frac{1+r_{pp}}{1-r_{pp}}\cos\theta_{\alpha 1}(Z - Z_U)\right] \quad (26)$$

and rearrange terms by moving all upcoming waves to the left-hand side

$$W'_U = W_U - S_{xw}X_U + S_{zw}Z_U = W - S_{xw}X + S_{zw}Z \quad (27)$$

where $S_{xw} = \alpha_1\rho_1\frac{1+r_{pp}}{\varepsilon}\sin\theta_{\alpha 1}$ and $S_{zw} = \alpha_1\rho_1\frac{1+r_{pp}}{1-r_{pp}}\cos\theta_{\alpha 1}$ (28)

W'_U is an effective upcoming pressure. Similarly for upcoming X, equation (25) can be solved for X component and rearranged so that the upcoming waves are at the left-hand side of the equation as

$$X'_U = X_U + S_{wx}W_U + S_{zx}Z_U = X + S_{wx}W + S_{zx}Z \quad (29)$$

where $S_{xz} = \frac{1-r_{pp}}{\varepsilon}\frac{\sin\theta_{\alpha 1}}{\cos\theta_{\alpha 1}}$ and $S_{wx} = S_{xw}^{-1}$ (30)

Finally, an effective upcoming Z will read

$$Z'_U = Z_U - S_{wz}W_U - S_{xz}X_U = Z - S_{wz}W - S_{xz}X \quad (31)$$

$$\text{where} \quad S_{wz} = S_{zw}^{-1} \quad \text{and} \quad S_{xz} = S_{zx}^{-1} \quad (32)$$

There are only upcoming waves separated and built up constructively on the left hand side of equation (26), (27) and (29) for each component. As a result, the downcoming waves are removed, leaving the effective upcoming waves. However, from these three equations, the total wavefields of any two components are scaled and summed into the third one with scalings designed to remove the downcoming waves. The remaining upcoming waves still contain these downcoming-scaling effects. For example, in order for Z_D and W_D to match and remove the downcoming X_D , the total Z and W are scaled with a downcoming-scaling factor for X , before combined to give the effective upcoming X'_U in equation (29). Therefore the results from these three equations are not exact value, but effective upcoming wavefields. The descaling factors for the upcoming waves in each component are to be computed as our future work. Nonetheless, from our numerical experiment, $\sin^2 \theta_{\alpha 1}$ is one of the descaling factors needed to stabilize the X'_U in equation (29) and $\cos^2 \theta_{\alpha 1}$ for Z'_U in (31).

RESULTS

To test the method, a multicomponent set of numerical OBC seismic models was generated by Elmo (Elastic Modelling), an in-house elastic modelling program based on the phase-shift cascade method (Silawongsawat and Margrave, 1998 and Silawongsawat, 1998). The program has been modified to generate 2-D multicomponent OBS data. A geological model in Figure 4 is used to synthesize a single source record.

The modelled pressure contains a total wavefield gather, an up- and a down-arrival gathers, which are displayed in Figure 3, 5 and 7 respectively. The estimation of upcoming pressure from the scalar combination method (in f - k domain), Figure 6, is then plotted beside the exact result from Elmo. It shows that the scalar combination has effectively removed the downcoming waves from the total pressure wavefield. Careful comparison will show that the upcoming estimate, W'_U , has subtle differences in amplitude from the modelled result, W_U .

For clearer demonstration, some traces of the synthetic total pressure gather from Figure 3, whose offsets are between -1000 and 1000 m. are plotted as wiggle traces in Figure 8, beside the synthetic downcoming pressure in Figure 7. On top of the traces in Figure 8, their corresponding estimation from the scalar combination of velocity components is marked with the same polarity to compare the downcoming events. Notice that an upcoming event between 0.7s - 0.9s has opposite polarity in this plot, consequently the subtraction of downcoming waves is constructive for the upcoming pressure. This shows that the method effectively matches the downcoming pressure produced from a combination of horizontal and vertical particle velocity and thus efficiently removes such unwanted signals. The desired upcoming wavefield which represents the subsurface information is then better resolved.

The similar successful downcoming-removal results of the method in vertical component, Z'_U , are displayed in Figure (10), compared to the input total wavefield, Z , in Figure (9). Assuming near offset, a trace plot in Figure (11) shows the X - W combination of the last two terms in Equation (31), plotted as a cross (+), matches perfectly to the total wavefield traces, Z which is the first term in the same equation. While the amplitudes of the downcoming waves have the same polarity, the upcoming waves opposite one. We also tested a conventional Z - W summation method used by Barr and Sanders (1989) in both Z and W components. It confirms the same results in both components and Figure (12) shows downcoming removals from Z - W summation method for vertical component in comparison to the Figure (10).

In the horizontal component, the scalar combination is also proved equally effective at eliminating the downcoming wavefield as illustrated in Figure (14). Compared to Figure (13) of the total wavefield, X , it is obvious that the firstbreak and the source-ghost are removed, leaving the subsurface information in the upcoming wavefield clearer shown in the result. Due to the downcoming scaling effect in the combined upcoming X'_U , we separately compare the scaled downcoming scalar combination and the descaled upcoming of the X -component in Figure(15) and (16), respectively. They show the downcoming X are very well matched and thus removed and the descaled upcoming results are well preserved.

CONCLUSION

Elmo synthesizes multicomponent OBS data correctly. It can also separately generate any responses, ie. up or down propagating waves, up or down arrivals, P or S waves, at above or below the seafloor, which is tremendously helpful to this research.

The commonly used technique relates the vertical particle velocity to pressure through a vector relationship derived from Newton's second law. Using Hook's law, we have derived an alternative scalar relation between pressure and all components of particle velocity.

Tests with synthetic data show that the method can effectively remove the downcoming pressure by subtracting a scalar combination of the velocity components. Vertical and horizontal velocity components are similarly process and successfully isolate their upcoming component.

ACKNOWLEDGEMENTS

We thank the CREWES sponsors for their support.

REFERENCES

- Aki and Richards, P.G., 1980, Quantitative Seismology, W.H. Freeman & Co.
Amundsen, L., 1993, Wavenumber-based filtering of marine point-source data, *Geophysics*, **58**, 1335-1348.

- Barr, F.J., and Sanders, J.I., 1989, Attenuation of Water-Column Reverberations Using Pressure and Velocity Detectors in a Water-bottom cable, 59th Annual Internat. Mtg, Soc. Expl. Geophys., Expanded abstracts, 653-656.
- Dankbaar, J.W.M., 1985, Separation of P- and S-waves, *Geophys. Prosp.*, **33**, 970-986.
- Donati, M.S., and Stewart, R.R., 1996, P- and S-wave separation at a liquid-solid interface, *J. Seis. Expl.*, 113-127.
- Sheriff, R.E., and Geldart, L.P., 1995, *Exploration Seismology*, 2nd ed., Cambridge University Press.
- Silawongsawat, C, and Margrave, G.F., 1998, The Phase shift cascade method of elastic wavefield modelling: 68th Annual SEG Meeting, expanded abstracts, 1807-1810.
- Silawongsawat, C, 1998, Elastic wavefield modelling by Phase shift cascade, M.Sc. thesis, University of Calgary
- Silawongsawat, C. and Margrave, G.F., 1999, A proposal for suppression of downcoming waves at the ocean bottom with multicomponent data, CREWES annual research report.

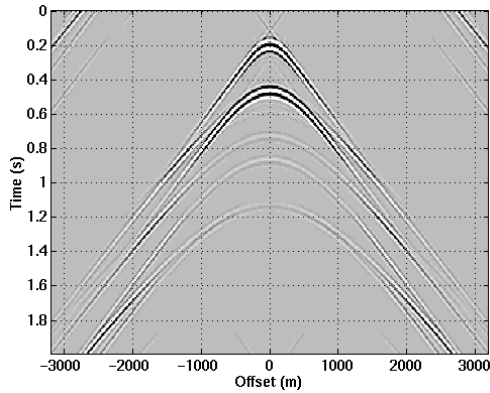


Figure 3. Numerically-generated total pressure wavefield W , both up- and down-traveling waves, arrive at hydrophones located just above the ocean bottom

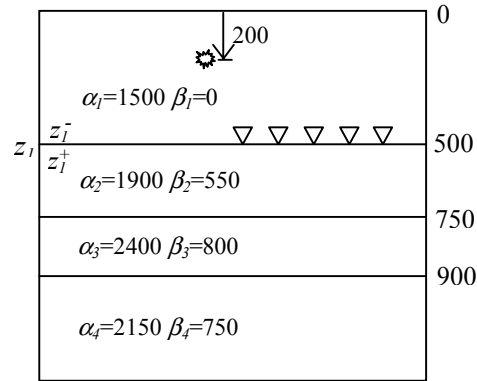


Figure 4. Geological model and survey configuration used for generating multi-component synthetic OBC seismograms

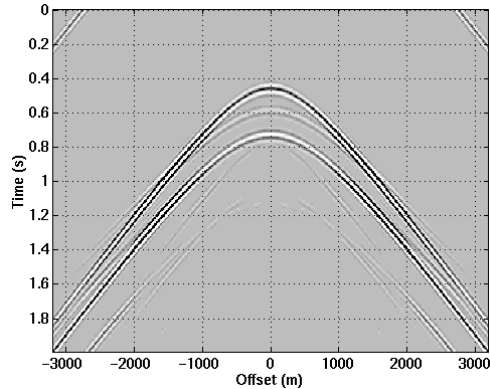


Figure 5. Upcoming pressure separately generated by Phase shift cascade method, W_U .

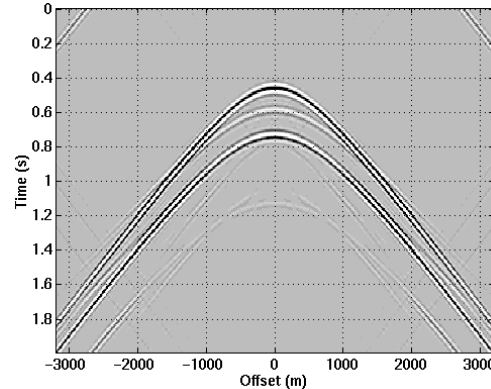


Figure 6. Upcoming pressure from multi-component scalar combination, W'_U .

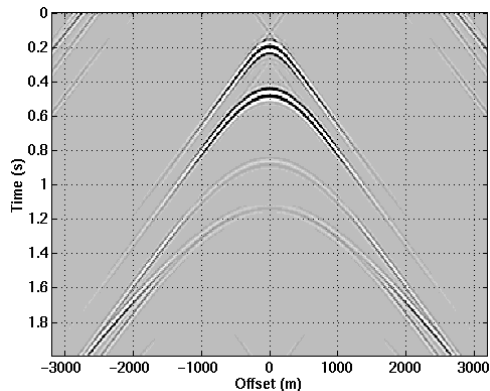


Figure 7. Separately generated downcoming pressure by Phase shift cascade, W_D .

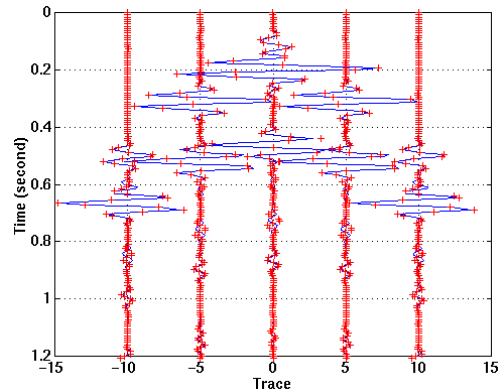


Figure 8. Selected total pressure traces, W , with their corresponding X - Z scalar combination plotted as a cross (+) on top in comparison.

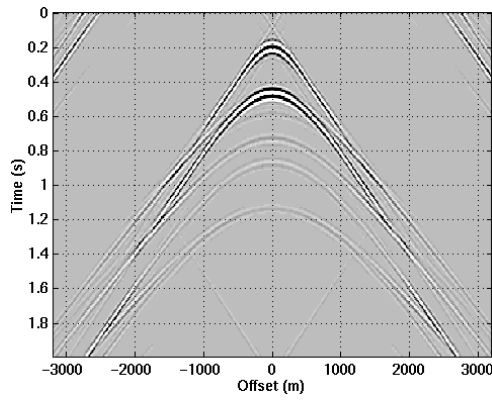


Figure 9. Synthetic total wavefield in vertical component, Z .

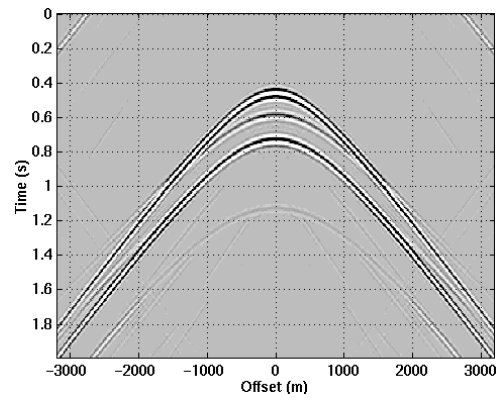


Figure 10. Effective upcoming waves in vertical component, Z'_U , separated by scalar combination method.

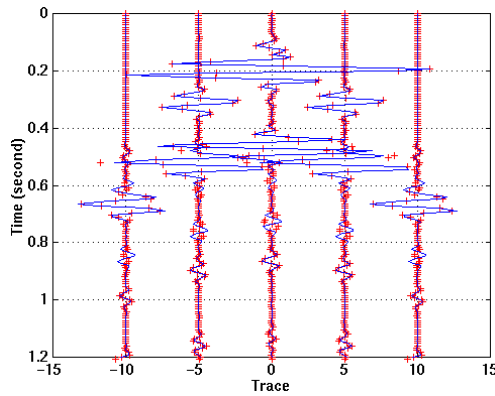


Figure 11. Total wavefield in vertical component traces, Z , with their corresponding $X-W$ scalar combination plotted as a cross (+) on top in comparison.

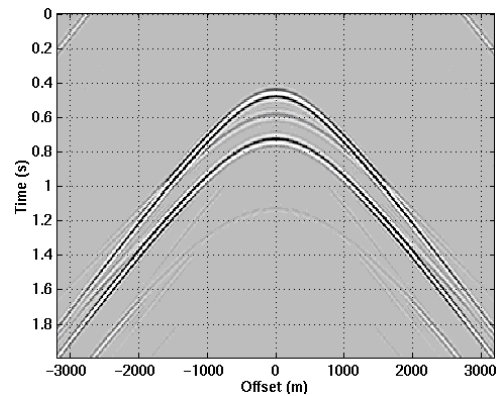


Figure 12. Upcoming vertical particle velocity, Z_U , computed by conventional $Z-W$ summation

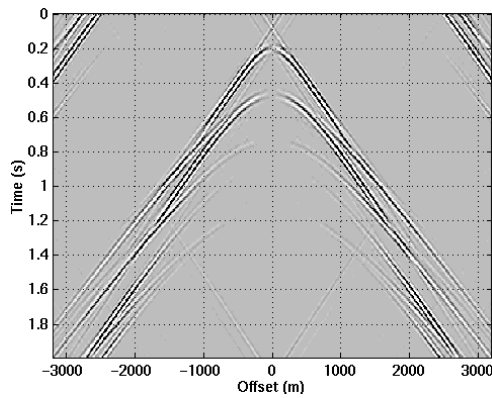


Figure 13. Synthetic total wavefield in horizontal component, X .

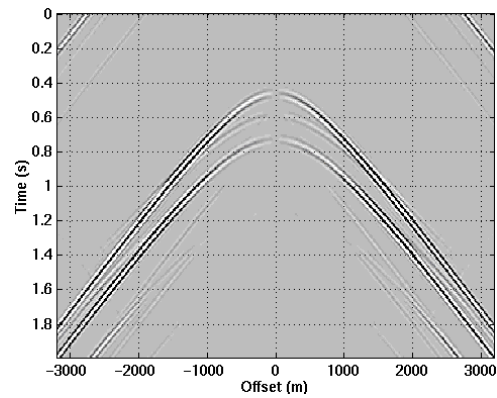


Figure 14. Upcoming horizontal-particle velocity from multicomponent scalar combination with a descaled factor, $\sin^2 \theta_{\alpha 1} X'_U$.

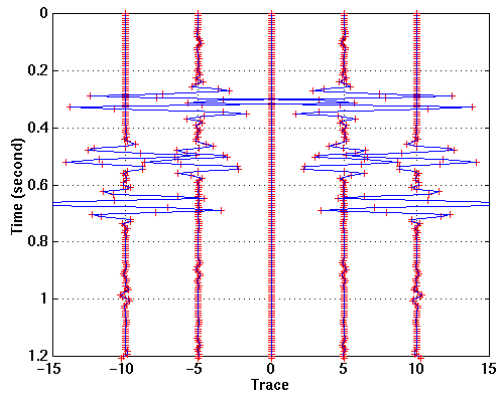


Figure 15. Synthetic downcoming waves in horizontal component traces, X_D , and their corresponding Z - W scalar combination, $(X'_U - X_U)$ from equation (27).

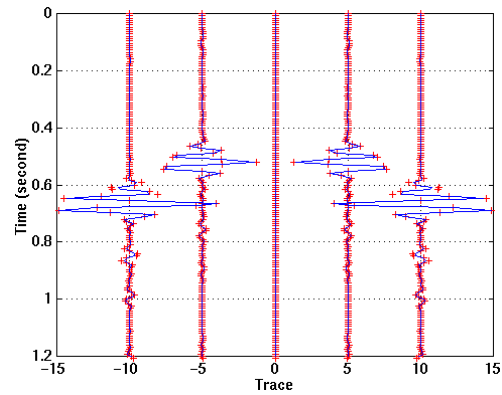


Figure 16. Synthetic upcoming waves in horizontal component traces, X_U , and their downcoming-descaled Z - W scalar combination, $\sin^2 \theta_{\alpha 1} (X'_U - X_U)$.